

Optimal Pacing of a Cyclist in a Time Trial Based on Experimentally Calibrated Models of Fatigue and Recovery

Faraz Ashtiani, *Student Member, IEEE*, Vijay Sarthy M Sreedhara, Ardalan Vahidi, *Senior Member, IEEE*, Randolph Hutchison, Gregory Mocko

Abstract—In this paper, we first report the use of experimental data from six human subjects to validate and calibrate our proposed dynamic models for fatigue and recovery of cyclists in [1]. These models are employed to formulate pacing strategy of a cyclist during a time trial as an optimal control problem. Via necessary conditions of Pontryagin Minimum Principle (PMP), we show that the cyclist’s optimal power is limited to four modes in a time-trial. To determine when to switch between them, we resort to numerical solution via dynamic programming. One of the subjects is then simulated on four courses including the 2019 Duathlon National Championship in Greenville, SC. The DP simulation results show reduced time over experimental results of the self-paced subject who is a competitive amateur cyclist.

I. INTRODUCTION

OPTIMIZATION of human performance by accurately modeling fatigue has challenged athletes, coaches, and scientists. The rise in popularity of wearable sensors in physical activity tracking presents opportunities for modeling and optimizing performance as they alleviate the need for expensive laboratory equipment. Understanding fatigue dynamics can potentially help athletes train in a more efficient way and perform at their peak. Moreover, it can provide useful information to further enhance the performance of an athlete during a physical exercise. Fatigue due to prolonged exercise is defined as a decline in muscle performance which accompanies a sensation of tiredness [2], [3]. Therefore, during physical exercise, fatigue prevents athletes from producing the required power. Several studies such as [4], [5] have investigated fatigue in cycling and developed models for it based on the expenditure of anaerobic energy. Only a few studies investigate the recovery dynamics of this anaerobic energy [6].

Figure 1 illustrates a cyclist pedaling in a time trial on a mountain course. Even seasoned cyclists may find it challenging to pace themselves in such a course. By over exerting themselves too early or too late, they may not achieve their maximum potential. We hypothesize that cyclists can finish a time trial faster if they plan in advance in consideration of

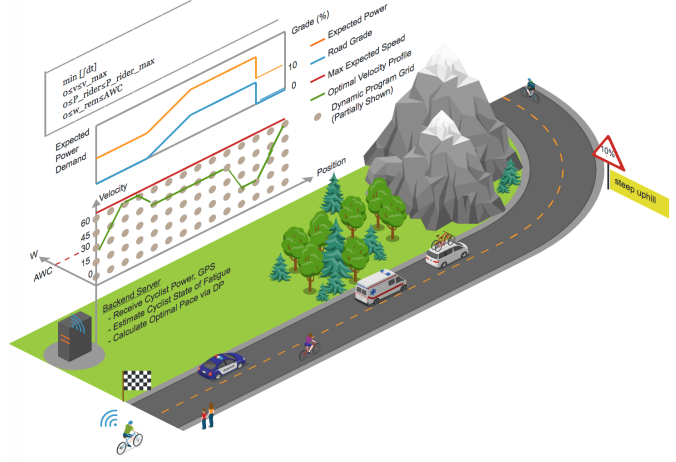


Fig. 1: An illustration of optimal pacing of a cyclist using upcoming elevation data, a dynamic model of cyclist fatigue and recovery, and a model of bicycle longitudinal dynamics. The illustration also shows a dynamic programming grid on two states of velocity and anaerobic energy for planning the optimal velocity or power. The optimal power is communicated and displayed to the cyclist in real-time. Drawn in <https://www.icograms.com>.

their Anaerobic Work Capacity (*AWC*) and upcoming road elevation. The pacing strategy can be formalized as an optimal control problem which requires dynamic models of fatigue and recovery and maximal power capacity of a cyclist as a function of their fatigue levels. While former members of our team had attempted optimal pacing based on a dynamic model of muscle fatigue and recovery in [7] and [8], such lumped muscle models were complex and hard to experimentally verify and calibrate. Alternatively, one can consider fatigue as running out of *AWC* which could be captured with a single dynamic state and recovery is achieved when pedaling below a Critical Power (*CP*). Such a model can be more easily verified and calibrated in laboratory experiments as our recent work in [1] and [9] shows. In fact, a model based on anaerobic energy expenditure has been used in [10] to optimize a 5 km cycling time-trial. However, a model for recovery was not considered in [10] perhaps because the road was assumed to be flat, not necessitating a more sophisticated strategy.

In this paper, the dynamic models for a cyclist’s fatigue and recovery during anaerobic exercise presented in [1] are further validated and calibrated for six human subjects using 14 hours of experiments per subject that we collected in the lab. We believe these models based on anaerobic work capacity are more practical to use in optimal pacing than those

(Corresponding author: Faraz Ashtiani)

Faraz Ashtiani (fashtia@g.clemson.edu), Vijay Sarthy M Sreedhara (vsreedh@clemson.edu), Ardalan Vahidi (avahidi@clemson.edu), and Gregory Mocko (gmocko@clemson.edu) are with the Department of Mechanical Engineering, Clemson University, Clemson, SC 29634-0921, USA. Randolph Hutchison (randolph.hutchison@furman.edu) is with the Department of Health Science, Furman University, Greenville, SC 29613-1000, USA.

based on estimating muscular fatigue presented in [7] and [8]. This is mainly because the state of AWC can be estimated rather reliably open-loop and by integrating the cyclist's power output over time and without the need for invasive (e.g. blood lactate) measurements. Furthermore, we show in this paper that affine dependence of system's dynamics and constraints on control input (pedaling power) allows for valuable analytical insights into the nature of optimal pacing strategy when using Pontryagin's Minimum Principle. We resort to numerical solution via Dynamic Programming (DP) to resolve the switching between various modes of optimal strategy. We simulate one of the subjects on four time-trial courses including the 2019 Greenville Duathlon National Championship.

Section II presents a literature review on muscle fatigue and recovery. Section III introduces our proposed mathematical models for anaerobic energy expenditure and recovery besides maximum power generation ability of cyclists. In Section IV the experimental protocol and results for six cyclists are presented. After developing the models we formulate the optimal pacing problem in Section V. The problem is investigated analytically in Section VI using optimal control theory, and numerical solutions using dynamic programming are shown in Section VII, followed by conclusions.

II. LITERATURE REVIEW

A. Fatigue Definition and Mechanism

Several studies have investigated fatigue, which has led to its many definitions. For example, in [11] authors define fatigue as a reduction in maximal capacity to generate force or power during exercise. Whereas, fatigue is defined as inability to produce the desired force or power resulting in impaired performance in [12] and [13]. The point of occurrence of fatigue is defined as the moment at which a drop from the desired power level is observed, which is also time-to-exhaustion, thus making both terms indistinguishable [14]. To address this, in [15] and [16] fatigue is defined as a continuous process altering the neuromuscular functional state resulting in exhaustion and exercise termination. In general, there are two sources of fatigue: central fatigue and peripheral fatigue [17]. Central fatigue is defined as the failure of the Central Nervous System (CNS) in sending necessary commands to muscles to operate [18]. This factor is essentially important in high-intensity exercise [19]. Peripheral fatigue is caused at the muscle level. It can be induced because of the neuromuscular failure in muscles to comprehend and perform the commands coming from CNS, and deficiency of vital substances [19].

The above mentioned studies illustrate the difficulty involved in arriving at a global definition of fatigue. The mechanism of fatigue leading to exhaustion are different for cycling, running, swimming, etc [20]. As we previously presented in [1], we define muscle fatigue and recovery in cycling as follows:

- *Fatigue*: Expending energy from anaerobic metabolic systems by pedaling above a critical power which results in a decrease of maximum power generation ability.
- *Recovery*: Recuperating energy into anaerobic metabolic systems by pedaling below the critical power which

TABLE I: Comparison between three metabolic systems that provide ATP for muscle contraction [28].

Metabolic system	Moles of ATP/min	Endurance time
Phosphagen system	4	8-10 seconds
Glycogen-lactic acid system	2.5	1.3-1.6 minutes
Aerobic	1	Unlimited (as long as nutrients last)

results in an increase of maximum power generation ability.

B. Muscle Fatigue Measurement and Modeling

Measuring the effect of central fatigue on muscle performance is a challenge since the the matter is highly subjective [21]. Most research efforts to objectively measure central fatigue are focused on measurement of Maximum Voluntary Contraction (MVC) [22–24]. In voluntary contraction of a muscle, the generated force is proportional to the muscle electrical activation [25]. A standard way of measuring muscle activity is via Electromyography (EMG) tests. During the test the amount of electric potential produced in muscles can be measured. Although studies such as [26] and [27] have shown the accuracy of EMG tests in measuring maximal and submaximal voluntary contractions, there is evidence of underestimating the muscle activation at high force levels [17]. Therefore, to point to the goal of the current study, EMG cannot provide accurate data for modeling a cyclist's fatigue and recovery.

In addition to central fatigue there are several sites for peripheral fatigue. To get a better understanding of fatigue at muscle level, we should focus on muscle metabolic system. Muscle contraction needs a source of energy to be executed and the fuel that provides this energy is adenosine triphosphate (ATP). When one phosphate radical detaches from ATP, more than 7300 calories of energy are released to supply the energy needed for muscle contraction [28]. After this detachment, ATP converts to adenosine diphosphate (ADP). When a human muscle is fully rested, the amount of available ATP is sufficient to sustain maximal muscle power for only about 3 seconds, even in trained athletes [28]. Therefore, for any physical activity that lasts more than a few seconds, it is essential that new ATP be formed continuously.

There are three metabolic systems which provide the needed ATP: Aerobic system , Glycogen-lactic acid system and Phosphagen system. Table I compares the three systems, in terms of moles of ATP generation per minute and endurance time at maximal rates of power generation. Utilization of these systems during physical activity is based on the intensity of the activity.

Cycling can fall in all categories above depending on the intensity of the exercise. Many people cycle for fun and get around cities. In this case they may only use their aerobic system which provides them with low amount of power which they can hold for a very long time. However, during high intensity cycling such as in a time trial, the human body will use the other two sources besides the aerobic system to provide enough energy for muscle contraction. This is important when hypothesizing mathematical models that describe muscle power generation in cycling. Later on, we discuss a method

to define a power limit below which the cyclists use their aerobic metabolic system that allows them to hold their power for long periods of time. However, there is limited energy to pedal above this power limit.

During aerobic exercise, muscles utilize the aerobic metabolic system to produce ATP. Oxygen plays a vital role in formation of ATP molecules. There are two major methods to measure oxygen during a fatiguing exercise. The first one is measuring the volume of oxygen intake in breathing ($\dot{V}O_2$) [29]. During a physical exercise, $\dot{V}O_2$ increases to provide the necessary oxygen needed to produce ATP in the muscle as suggested in [30], [31], and modeled in [32]. The experimental procedure to measure $\dot{V}O_2$ requires a number of laboratory equipment that cannot be used by a cyclist during everyday outdoor ride. The second method is directly measuring the amount of oxygenated hemoglobins at the local muscle (muscle oxygenation). When muscles are fully fresh, the percentage of oxygenated hemoglobins among the total number of hemoglobins is at its highest. During a fatiguing exercise, this percentage drops. Several studies show that Near Infrared Spectroscopy (NIRS) is a robust method to measure muscle oxygenation [33–35]. A few companies currently make wearable devices that enable the cyclists to monitor their muscle oxygenation in real-time [36], [37]. We have shown in [1] a real-time measurement of muscle oxygenation during a set of experiments.

Another fatigue indicator is the amount of lactate produced in the muscle. Maximum Lactate at Steady State (MLSS) is the maximum maintainable blood lactate concentration without additional buildup through aerobic exercise [38], [39]. During an anaerobic exercise, the rate of lactate production is higher than its dissipation [40], [41]. As authors in [42] and [43] suggest, the amount of lactate accumulation can provide useful information about the fatigue level of muscles. The high lactate levels at muscle represent a lower ability of the muscle to generate force and power [12], [44], [45]. Traditionally, a common way to measure lactate has been taking blood samples or biopsies during an experiment [46], [47]. These invasive methods are not in any way suitable for a real-time measurement and estimation of fatigue. Recently, authors in [48] developed a non-invasive method to measure blood lactate using electromagnetic wave sensors. Commercialization of such non-invasive in-situ measurement techniques will enable researchers to develop mathematical models that represent the relationship between blood lactate level and muscle power/force generation capacity.

C. Fatigue in Cycling

In cycling, it is easier to measure power without elaborate laboratory equipment owing to the development of commercial grade power meters. A power meter can be used for training, developing pacing strategies for a time trial, and performance evaluation after an exercise or race [49]. However, determining exercise intensity using power is not straightforward as a threshold power is needed to classify exercise intensity. As stated in [50] and [51], the Critical Power (CP) can potentially be used to determine exercise intensity. It has been shown that

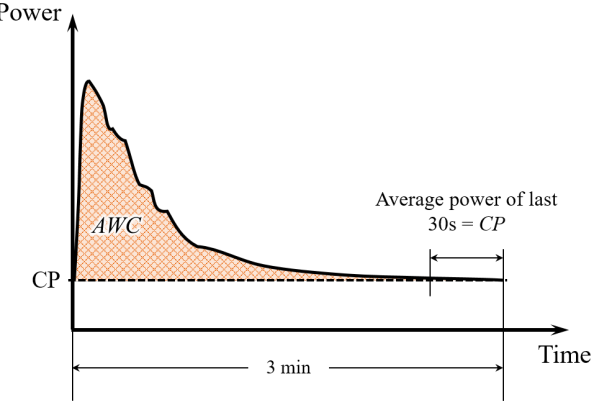


Fig. 2: The 3-minute-all-out test protocol. The average power at the last 30 seconds of the tests is considered to be CP , and the area between power plot and CP is equivalent to AWC .

CP is close to the power at which MLSS occurs according to [52–54]. This means, while pedaling at a power level above CP , a cyclist would expend energy from anaerobic energy sources. On the other hand, pedaling below CP helps the cyclist replenish its anaerobic reserve [52–54].

The critical power concept was introduced by authors in [55]. They defined CP as the maximum power output that can be maintained indefinitely. In [56] authors showed that there is a limited amount of anaerobic energy for a cyclist to pedal above CP . This “tank” of energy is called *Anaerobic Work Capacity* (AWC). They suggest by pedaling at a certain power level above CP , a cyclist can hold that power for a limited amount of time before he or she runs out of anaerobic energy. This is known as the *two parameter model*. The relationship between critical power and anaerobic work capacity is often expressed as:

$$P = CP + \frac{AWC}{t_{lim}} \quad (1)$$

where P is instantaneous power in Watts, and t_{lim} is time-to-exhaustion in seconds. The experimental protocol designed to calculate CP and AWC in Equation (1) requires multiple lab visits for the test subjects according to [5], [57–60].

To avoid these multiple lab visits, authors in [61] developed a 3-minute-all-out test (3MT) as in Figure 2. In this test, subjects sprint “all-out” for the entire 3 minutes. The value of CP is given by the average power output of the last 30 seconds. The value of AWC is the area between the power curve and CP . This test has been further validated in [62] and [63]. However, there are some recent papers arguing the validity of the 3MT test to estimate CP and AWC [64], [65]. In [64] authors suggest that while 3MT provides an over estimate of CP , it can still be considered as a useful test since it reduces the number of lab visits significantly. For the purpose of this paper, we rely on the 3MT test to determine CP and AWC .

III. MODELING FRAMEWORK

As discussed in Section II-C, AWC is a finite energy store for pedaling above CP . When a cyclist expends his or her

AWC entirely, the maximum power that can be produced is *CP*. Let *w* be the amount of *AWC* remaining. The rate of change of *w* while expending energy above *CP* is given by the difference between the rider's power and *CP*. Recovery rate can be calculated similarly as assumed in [66]. However, it has been shown in [67] and [68] that recovery occurs at a slower rate than expenditure. For instance, if the cyclist is pedaling at a power level below the critical power, the actual amount of recovered energy (*w_{rec}*) will be less than the area between *CP* and the power curve. Thus, we propose to compute an adjusted recovery power using *w_{rec}* given by,

$$P_{adj} = CP - \frac{w_{rec}}{T_{rec}} \quad (2)$$

where *P_{adj}* is the adjusted recovering power, and *T_{rec}* is the duration of recovery. Equation (2) can be rewritten to form an energy expenditure and recovery model as,

$$\frac{dw}{dt} = \begin{cases} -(P - CP) & P \geq CP \\ -(P_{adj} - CP) & P < CP \end{cases} \quad (3)$$

where *P* is the power output of the cyclist.

Equation (3) represents a switching dynamic model of fatigue and recovery. To calculate the adjusted power we need a model that can provide *P_{adj}* at any power level in the recovery interval (i.e. below *CP*). One of the assumptions of this study is that the recovery rate of *w* does not depend on the duration of the recovery interval *T_{rec}*. This assumption stems from the need for a causal energy recovery model. If it is assumed that *w*'s rate of recovery depends on *T_{rec}*, the amount of recovered energy during recovery interval will depend on the recovery duration in the future which does not seem plausible. In our previous study in [1], we elaborated more on the reason behind making this assumption by using muscle oxygenation data.

To arrive at a relationship between *P_{adj}* and the actual applied power by the rider, *P_{adj}* calculated from the tests at each recovery power is plotted against the actual pedaling powers, and the following linear model provides a good fit to the data we present later in the paper,

$$P_{adj} = aP + b \quad (4)$$

where *a* and *b* are the model's constants.

Another parameter which is affected by the expenditure of *AWC* is the cyclist's ability to generate an instantaneous maximum power at any point during cycling. Previously in [1], we've shown a linear relationship between maximum power and remaining anaerobic energy during a 3MT test. Additionally, through a series of short sprints, several studies [69–71] have shown that the pedaling speed (cadence) affects the maximum power generation ability of a cyclist regardless of his or her state of fatigue. The maximum power is a second order parabolic function of cadence as in,

$$P_{max} = -\left(\frac{4P_{peak}}{\omega_{max}^2}\right)\omega^2 + \left(\frac{4P_{peak}}{\omega_{max}}\right)\omega \quad (5)$$

where *P_{peak}* is the peak power of the parabolic function, *ω*

is the cyclist's cadence, and *ω_{max}* is the cyclist's maximum cadence, which is reached when *P_{max}* = 0.

Other studies also investigate the effect of fatigue of this parabolic relationship [72–74]. In [74] the authors show that if we repeat the short sprint test at different anaerobic energy levels and plot the parabolic function, the peak powers have a linear relationship with their respective remaining anaerobic energy. This is similar to our previous findings in [1] where we propose a linear maximum power model as,

$$P_{peak} = \alpha w + CP \quad (6)$$

where *α* is the constant of the model. Similar to power, maximum cadence also decreases with fatigue [72], [74]. As authors show in [74], maximal cadence is a linear function of the remaining anaerobic energy (*w*),

$$\omega_{max} = \alpha_w w + \omega_{max,f} \quad (7)$$

where *α_w* is a model parameter and *ω_{max,f}* is the maximum cadence of the cyclist when *AWC* is fully depleted. Therefore, we can update Equation (5) using Equations (6) and (7) as below,

$$P_{max} = -\left(\frac{4(\alpha w + CP)}{(\alpha_w w + \omega_{max,f})^2}\right)\omega^2 + \left(\frac{4(\alpha w + CP)}{(\alpha_w w + \omega_{max,f})^2}\right)\omega \quad (8)$$

IV. EXPERIMENTAL PROTOCOL AND RESULTS

The experimental protocol comprised of three tests namely, (i) a ramp test to determine \dot{V}_{O_2} and Gas Exchange Threshold (GET), (ii) a 3-minute all-out test (3MT) to determine *CP* and *AWC*, and (iii) an interval cycling test to determine the recovery of *AWC*. The ramp test involves incrementally increasing the power until the subject is exhausted. From the ramp test, oxygen uptake \dot{V}_{O_2} , defined as the volume of oxygen inhaled per minute per kilogram of body weight [29], is determined. Furthermore, during the test, there is an abrupt change in the ratio of volume of CO_2 exhaled to the volume of O_2 inhaled, which is the point at which blood lactate concentration starts to increase. The power at \dot{V}_{O_2} (maximum oxygen uptake) and GET are recorded to aid in designing the 3MT test. The *CP* and *AWC* from the 3MT are also used to design the interval test for modeling the *AWC* recovery. The experimental protocol was approved by the Institutional Review Board of Clemson and Furman Universities. Besides power, muscle oxygenation and heart rate were also recorded during the tests. The interval test was developed using the definitions of fatigue and recovery from Section II-A to derive mathematical models for recovery of *AWC* as well as the maximum power generation capacity of cyclists at any instant in a ride. The protocol was developed under the following assumptions:

- The 3MT test provides reliable estimates of *CP* and *AWC*.
- Exercise below *CP* utilizes the aerobic energy source, and results in recovery of *AWC*.

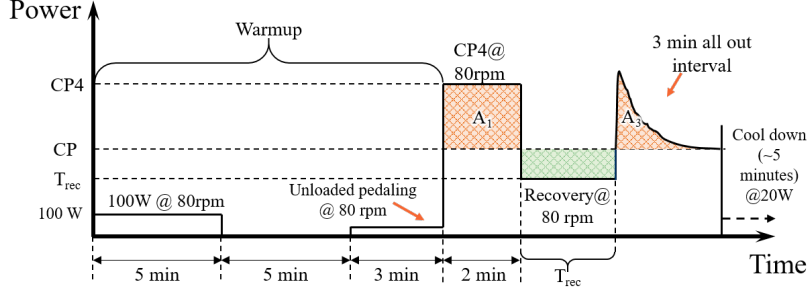


Fig. 3: The power interval test protocol. After a warm-up period, the subject pedals at CP_4 for 2 minutes. Then the cyclist pedals at three different recovery power levels for different time intervals to recover energy. Following that, the subject performs a 3-min-all-out to burn all the remaining energy from AWC .



Fig. 4: A view of the testing environment. The cyclist in this photo is not one of our subjects.

- The recovery of AWC below CP happens at a slower rate than its expenditure above CP .
- The rate of recovery depends on the recovery power and not the duration of recovery.
- The power held during recovery interval is averaged and assumed to be constant.

We have conducted experiments on a total of 17 subjects. All of the subjects are cyclists who cycle at least 3 times a week, and are used to high intensity workout sessions. Each subject was scheduled for 14 hour-long visits to our laboratory. Because of the complexities of such scheduling, only 6 of them were able to finish all of the tests. The test protocol was approved by Clemson University's Institutional Review Board (IRB) under protocol numbers IRB2016-169 and IRB2017-222. In order to be compliant with IRB policies we label our subjects by a number. The subjects who successfully finished all the experiments were Subs 6, 9, 11, 12, 14, 16.

All tests were conducted in a laboratory setting on both Clemson and Furman University campuses. The tests were programmed on a RacerMate CompuTrainer [75] using Perf-pro studio software application [76]. There are some studies such as [77] that suggest the CompuTrainer's power measurement accuracy depends on a variety of parameters such as temperature and calibration procedure. Nevertheless, the

TABLE II: Experimentally determined parameters for the six subjects who successfully finished all of the 3-min-all-out and interval tests.

Subject	Sex	m (kg)	CP (Watts)	AWC (J)	a	b (Watts)	α (1/s)	α_C (rpm/J)	$\omega_{max,f}$ (rpm)
6	M	79	269	12030	0.11	237.5	0.037	0.017	139
9	M	63	233	10100	0.09	204.5	0.036	0.014	158
11	M	95	335	15092	0.08	300.9	0.039	0.01	163
12	M	70	217	5637	0.12	196.5	0.046	0.009	142
14	F	74	242	7841	0.08	222.5	0.044	0.008	164
16	M	51	206	9137	0.2	167.5	0.025	0.007	154

CompuTrainer has been shown to be a valid device to estimate CP and AWC using the 3MT test [78] and [79]. Figure 4 shows the experimental setup in our laboratory. On the first visit, the ramp test was conducted followed by a 3MT familiarization test. On the next three subsequent visits, a fresh 3MT was conducted from which we can calculate the average CP and AWC . On the fifth visit, the interval test familiarization was conducted. On the subsequent visits, the interval tests at three different recovery powers (min power on Computrainer 80 Watts, 90% of power at GET (P_{GET}), and half way between P_{GET} and CP) and three durations (2 min, 6 min, 15 min) were conducted. The power levels are adopted from [80] and recovery durations from [67]. There was at least 24 hours between two consecutive tests to ensure complete recovery. In the interval test protocol as shown in Figure 3, after a warm up of 10 minutes, there is a 2 minute interval at CP_4 , the power at which all of the subject's AWC will be consumed in 4 minutes ($CP_4 = \frac{AWC}{240}$). The subject expends 50% of their AWC in the 2-min CP_4 interval and then recovers AWC at the mentioned recovery powers and durations. Following the recovery interval, the subject then performs a 3-min-all-out test to expend all of their remaining AWC . The amount of energy recovered in the recovery interval is then determined by subtracting AWC from the summation of areas above CP through the entire test.

It should be noted that we hypothesized Equation (8) after we collected our experimental data. Therefore, we made an assumption for us to be able to determine the constants α , α_C and $C_{max,f}$ post hoc. We assume the braking force applied by the CompuTrainer is set in a way that the subject is always at the peak power of the parabolic power-cadence function at each energy level in figure 6. Under this assumption we will be able to determine the model constants in Equation (8) with a single 3MT.

In order to find the recovery model parameters, the results

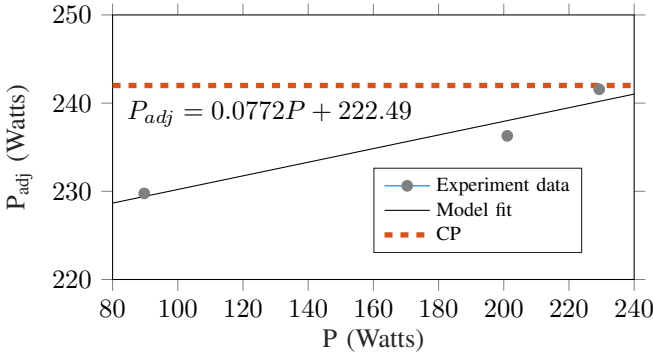


Fig. 5: Recovery model plot for Sub 14.

of the interval tests are analyzed. As mentioned in Section III, it is assumed that the recovery model doesn't depend on time interval. Therefore, at each power level below CP , the adjusted power is calculated for the 3 time intervals and then averaged. By doing this we will have a plot of adjusted power versus actual applied power, consisting of 3 data points. Figure 5 represents the recovery model derived for Sub 14. Each of the three data points in this figure represents the average adjusted power at each recovery power level for all three time intervals. The data point close to CP represents the adjusted power for the case where the subject pedals at halfway between GET and CP . Since the corresponding adjusted power is very close to CP we expect very little energy recovery at this level.

The summary of modeling results for all of the subjects is presented in Table II. The reported values for CP , AWC , and constant parameters of the Equation (8) are the average of the three 3MT tests each subject performed. An interested reader can find more information about the quality of fit in reference [9].

Figure 6 visualizes Equation (8) using Sub 14's model parameters which will later be used in our optimal control formulation as a constraint.

V. OPTIMAL CONTROL FORMULATION

In this section, the control problem formulation is discussed. The system has three states: i) traveled distance s ii) velocity of the bicycle v and iii) remaining energy of the cyclist w , and a single input which is rider's power u ,

$$\dot{x} = f(x(t), u(t)) = [f_1 \quad f_2 \quad f_3]^T \quad (9)$$

in which

$$x(t) = [s(t) \quad v(t) \quad w(t)]^T \quad (10)$$

where $x(t)$ is the states vector. The function f is the nonlinear state-space model function, which relates the rate of change of the 3 states to the states and input. The first state function f_1 in Equation (9) is simply,

$$\frac{ds}{dt} = v \triangleq f_1 \quad (11)$$

Newton's second law can be used to write,

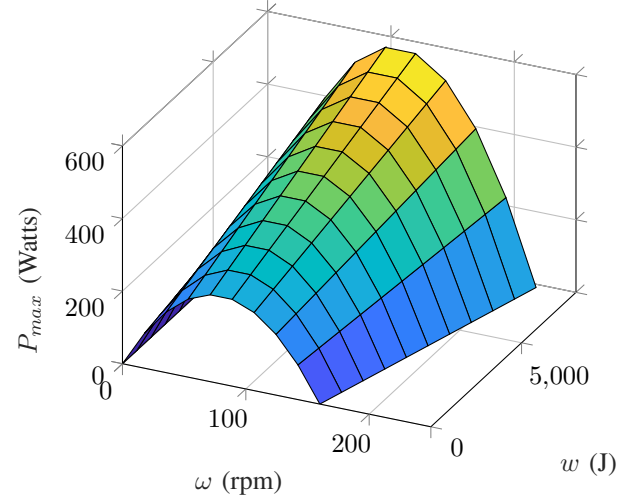


Fig. 6: Maximum instantaneous power as a function of the cyclist's cadence and remaining anaerobic energy.

$$\frac{dv(t)}{dt} = \frac{u(t)}{mv(t)} - \frac{m_b}{m} g(\sin(\theta) + C_R \cos(\theta)) - \frac{1}{2m} C_d \rho A v(t)^2 \triangleq f_2 \quad (12)$$

where m_b is the mass of the bicycle and rider, m is the effective mass which is 1.4% greater than m_b , C_d is the aerodynamic drag coefficient, A is the frontal area, ρ is the density of air which is assumed to be constant and independent of the elevation, θ is the road slope which is positive for uphill and negative for downhill, and C_R is the coefficient of rolling resistance of the road.

Assuming 100% efficiency for the bicycle powertrain, we can equate $u(t)$ to the cyclist's power on the pedals. The advantage of using Equation (12) is that gear selection is not a factor in our formulation, which otherwise makes the optimization more complex. Note that the third state equation for time derivative of cyclist's remaining anaerobic energy is the previously represented Equation (3),

$$f_3 \triangleq \frac{dw}{dt} = \begin{cases} -(u - CP) & u \geq CP \\ -((au + b) - CP) & u < CP \end{cases} \quad (13)$$

Now we are able to formulate a minimum-time optimal control problem to formalize the pacing strategy in a time-trial. Therefore, the objective function to be minimized is time,

$$\min_{u(t)} J = \int_{t_0}^{t_f} dt \quad (14)$$

subject to,

$$\begin{array}{ll} \text{state-space model:} & \dot{x} = f(x(t), u(t)) \\ \text{velocity limits:} & 0 \leq v(t) \leq v_{max} \\ \text{remaining energy limits:} & 0 \leq w(t) \leq AWC \\ \text{rider's power limit:} & 0 \leq u(t) \leq u_{max}(w, \omega) \end{array} \quad (15)$$

where u_{max} is defined by Equation (8). In this formulation the final position is specified and fixed but the other two states v and w are let open at the final position. In the simulations of this paper, we assume the maximal speed v_{max} is constant during the trip, but our approach applies if v_{max} varies along the road for example during sharp corners.

VI. NECESSARY CONDITION FOR OPTIMAL SOLUTION

In this section we study the defined optimal control problem using the variational approach. According to Pontryagin's Minimum Principle (PMP), the necessary condition for the optimality of input u is that it minimizes the following Hamiltonian function,

$$H(x(t), u(t), \lambda(t)) = L(x(t), u(t)) + \lambda^T(t) \{f(x(t), u(t))\} \quad (16)$$

in which

$$\lambda = [\lambda_1 \quad \lambda_2 \quad \lambda_3]^T \quad (17)$$

where λ is the vector of co-state variables, L is the integrand in the cost function J in (14), and f is the vector on the right hand side of the state equations with components represented in Equations (11), (12), and (13). We also need to address the constraint of maximum power generation of the cyclist. The maximum power u_{max} is a function of state variable w and cadence ω as represented in (8). We need to translate ω to the state variable v for the constraint to be applicable in our formulation. Using the gear ratio of the bicycle in our experimental setup, we can write the bicycle's velocity v at each gear as,

$$v(t) = g_i R_{rear} \omega \quad (18)$$

where g_i is the gear ratio of the i^{th} gear, and R_{rear} is the rear wheel (tire thickness included) radius. The lab's bicycle has 21 gear combinations which means we will have 21 plots like Figure 6 with different maximum velocities. We take the maximum surface of all of these 21 plots and create the constraint surface as shown in Figure 7.

Therefore, we observe an inequality constraint as a function of the control u , the state v and the state w variables. We can rewrite the constraint in a standard form as,

$$C(w, u) = u(t) - u_{max}(v(t), w(t)) \leq 0 \quad (19)$$

where $u_{max}(v, w)$ is defined by the surface in Figure 7.

In the presence of such an inequality constraint on control and state variables, the Hamiltonian equation needs to be augmented as follows [81],

$$H = L + \lambda^T f + \mu C \quad (20)$$

where

$$\mu \begin{cases} \geq 0 & C = 0 \\ = 0 & C < 0 \end{cases} \quad (21)$$

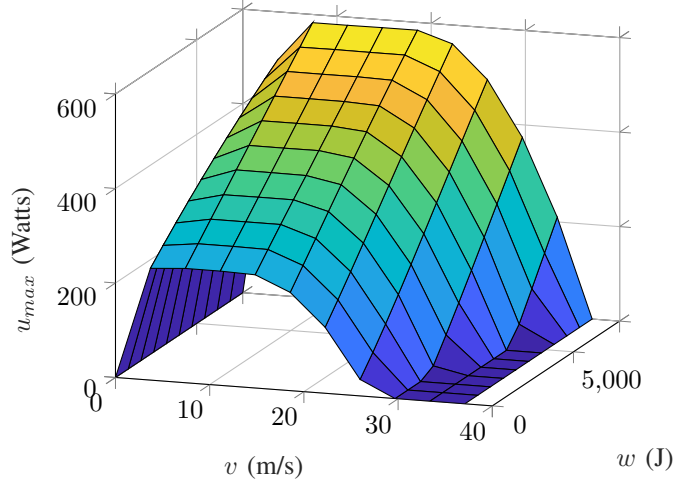


Fig. 7: The constraint surface on the control input u as a function of the state variables v and w .

Additionally, the upper and lower limits on v and w presented in Equation (15) should be taken into account as,

$$S(v, w) = \begin{bmatrix} v(t) - v_{max} \\ -v(t) \\ w(t) - AWC \\ -w(t) \end{bmatrix} \leq \vec{0} \quad (22)$$

According to [81], when constraints are not functions of the control input u , we take successive time derivatives of $S(v, w)$ and replace \dot{v} and \dot{w} with f_2 and f_3 , respectively, until we obtain an expression that is explicitly dependent on u . In this case, the first derivative of $S(v, w)$ with respect to both v and w includes u . Then, we can treat $S^{(1)}(v, w)$ just as $C(v, w)$ and augment the Hamiltonian as,

$$H = L + \lambda^T f + \mu C + \eta^T S^{(1)} \quad (23)$$

where $\eta = [\eta_1 \quad \eta_2 \quad \eta_3 \quad \eta_4]^T$ must obey the following conditions,

$$\eta_i \begin{cases} \geq 0 & S_i^{(1)} = 0 \\ = 0 & S_i^{(1)} < 0 \end{cases} \quad \text{for } i = 1, 2, 3, 4 \quad (24)$$

It should be noted that the terms μC and $\eta^T S^{(1)}$ will always be zero in the Hamiltonian when constraints are met. The dynamics of the co-states follow,

$$\dot{\lambda}^T = -H_x \equiv -L_x - \lambda^T f_x - \mu C_x - \eta^T S_x^{(1)} \quad (25)$$

where the subscript x denotes the partial derivative with respect to the corresponding state variables. Rider's remaining energy model in Equation (13) switches between fatigue and recovery conditions. Therefore, we have a switching Hamiltonian function between fatigue and recovery modes.

A necessary condition for optimality is that the control input u , minimizes the Hamiltonian. One can set the partial derivative of H with respect to u equal to zero. However, in

this case because H is affine in u , the derivative with respect to u (H_u) does not depend on u .

$$H_u = \begin{cases} \frac{\lambda_2}{mv} - \lambda_3 + \frac{1}{mv}(\eta_1 - \eta_2) + (\eta_4 - \eta_3) + \mu & u \geq CP \\ \frac{\lambda_2}{mv} - a\lambda_3 + \frac{1}{mv}(\eta_1 - \eta_2) + (\eta_4 - \eta_3) & u < CP \end{cases} \quad (26)$$

Note that the μ term only shows up when $u \geq CP$ because when $u < CP$ the constraint C is not active. Since Equation (26) does not depend on u , the optimal solution will be of the bang-singular-bang form; that is the Hamiltonian is minimized at extreme values of u with the exception of potential singular arcs in between.

When the Hamiltonian is affine in u , the sign of the H_u indicates the optimal input value. As is shown in Equation (26), the sign of H_u depends on μ and η . When μ has a non-zero (positive) value, the constraint C in Equation (15) is active which means the optimal value for u is its maximum (u_{max}) regardless of the sign of the slope. When either η_1 or η_2 has a non-zero value, $S_1^{(1)}$ or $S_2^{(1)}$ is active. In that case, it can be shown that acceleration should be zero which means the optimal value for u is the power at which velocity is constant ($u_{\dot{v}=0}$). When either η_3 or η_4 has a non-zero value, $S_3^{(1)}$ or $S_4^{(1)}$ is active. In this case, it can be shown that \dot{w} is zero which means the optimal input u will be at CP . The only cases left are when μ and η are all zero and we can cross them off from Equation (26) and rewrite it as,

$$H_u = \begin{cases} \frac{\lambda_2}{mv} - \lambda_3 & u \geq CP \\ \frac{\lambda_2}{mv} - a\lambda_3 & u < CP \end{cases} \quad (27)$$

The system of equations that should be solved are the state-space Equations (9) and (25), which provide 6 equations combined. The expanded version of the Equation (25) will be,

$$\begin{cases} \dot{\lambda}_1 = g\lambda_2 g\theta'(s)(\cos(\theta(s)) - C_R \sin(\theta(s))) \\ \dot{\lambda}_2 = -\lambda_1 + \frac{\lambda_2}{m_t} \left(\frac{u}{v^2} + C_d \rho A v \right) \\ \dot{\lambda}_3 = 0 \end{cases} \quad (28)$$

Now let's compare the H_u in both fatigue and recovery modes. If the H_u is positive, the minimum value of u minimizes the function. On the other hand, if the H_u is negative, the maximum value of u minimizes the function. We can consider four cases,

Case I: $\frac{\lambda_2}{mv} - \lambda_3 < 0$ AND $\frac{\lambda_2}{mv} - a\lambda_3 < 0$

The slope in both fatigue and recovery modes are negative which means maximum value of u in each case minimizes the Hamiltonian. Now, we should see which one results in a lower value of Hamiltonian. In the fatigue mode the maximum input value is u_{max} , and in the recovery mode the maximum input value is CP ,

$$H^* = \min \{H_{\text{fatigue}}(u_{max}), H_{\text{recovery}}(CP)\} \quad (29)$$

where the subscripts of H differentiates between fatigue and recovery modes because the equations of the two modes are slightly different. If we substitute the aforementioned values of u we cannot decisively say which Hamiltonian is smaller. We can write the optimal input as,

$$u^* = \begin{cases} u_{max} & H_{\text{fatigue}}(u_{max}) < H_{\text{recovery}}(CP) \\ CP & H_{\text{fatigue}}(u_{max}) > H_{\text{recovery}}(CP) \end{cases} \quad (30)$$

It should be noted that if the Hamiltonian is equal in both fatigue and recovery modes, we will have two optimal solutions.

Case II: $\frac{\lambda_2}{mv} - \lambda_3 > 0$ AND $\frac{\lambda_2}{mv} - a\lambda_3 > 0$

In this case, the input should take its minimum value in both cases, which will be CP and 0 for fatigue and recovery modes, respectively. The minimum Hamiltonian can be found from,

$$H^* = \min \{H_{\text{fatigue}}(CP), H_{\text{recovery}}(0)\} \quad (31)$$

The optimal input value in this case will be:

$$u^* = \begin{cases} CP & H_{\text{fatigue}}(CP) < H_{\text{recovery}}(0) \\ 0 & H_{\text{fatigue}}(CP) > H_{\text{recovery}}(0) \end{cases} \quad (32)$$

Similar to the previous case, if the Hamiltonian is equal in both modes, we will have two optimal solutions.

Case III: $\frac{\lambda_2}{mv} - \lambda_3 > 0$ AND $\frac{\lambda_2}{mv} - a\lambda_3 < 0$

In this case, the input takes its minimum value in fatigue mode, and its maximum value in recovery mode. In both of these scenarios the input is CP , so we can decide,

$$u^* = CP \quad (33)$$

Case IV: $\frac{\lambda_2}{mv} - \lambda_3 < 0$ AND $\frac{\lambda_2}{mv} - a\lambda_3 > 0$

In this case, the input takes its maximum value in fatigue mode, and its minimum value in recovery mode, which will be u_{max} and 0, respectively. The minimum Hamiltonian can be found from,

$$H^* = \min \{H_{\text{fatigue}}(u_{max}), H_{\text{recovery}}(0)\} \quad (34)$$

The optimal input value in this case will be:

$$u^* = \begin{cases} u_{max} & H_{\text{fatigue}}(u_{max}) < H_{\text{recovery}}(0) \\ 0 & H_{\text{fatigue}}(u_{max}) > H_{\text{recovery}}(0) \end{cases} \quad (35)$$

So far the optimal control input can take values of 0, CP , $u_{\dot{v}=0}$, and u_{max} . This means, when needed, the cyclist should recover at zero power. A hypothetical recovery scenario can be when the cyclist is on a steep downhill. However, there is still another case that is not investigated, which is a possible singularity condition.

Singular Arc: $\frac{\lambda_2}{mv} - \lambda_3 = 0$ OR $\frac{\lambda_2}{mv} - a\lambda_3 = 0$

Here we present the calculation for the case where the Hamiltonian's slope in the recovery or fatigue mode is zero.

It can be shown that we get the exact same final result for both modes. Therefore, we proceed with the recovery mode. During the possible singular condition in recovery mode we have,

$$\frac{\lambda_2}{mv} - a\lambda_3 = 0 \quad (36)$$

This equality needs to hold for an interval of time for a singular interval to exist. Therefore, its time derivative during that interval should also be zero. Setting the time derivative equal to zero and observing from Equation (28) that $\dot{\lambda}_3 = 0$ we get,

$$\frac{\dot{\lambda}_2}{v} - \frac{\lambda_2}{v^2}\dot{v} = 0 \quad (37)$$

We can substitute $\dot{\lambda}_2$ and \dot{v} from Equations (28) and (12), respectively:

$$\begin{aligned} \frac{1}{v} \left[-\lambda_1 + \lambda_2 \frac{u}{mv^2} + \frac{\lambda_2}{m} (C_d \rho A) v \right. \\ \left. - \frac{\lambda_2}{v} \left(\frac{u}{mv} - h(s) - \frac{1}{m} (C_d \rho A) v^2 \right) \right] = 0 \end{aligned} \quad (38)$$

Simplifying the equation above by using (36) yields,

$$\lambda_1 + am\lambda_3 h(s) + \frac{3}{2} (C_d \rho A) a \lambda_3 v^2 = 0 \quad (39)$$

Since input u does not appear in Equation (39), it becomes necessary to take the time-derivative again which yields,

$$\begin{aligned} -\dot{\lambda}_1 + am\dot{\lambda}_3 h(s) + am\lambda_3 \frac{dh}{ds} v \\ + \frac{3}{2} a \dot{\lambda}_3 (C_d \rho A) v^2 + 3a\lambda_3 (C_d \rho A) v \dot{v} = 0 \end{aligned} \quad (40)$$

Simplifying by using Equation (28) yields,

$$3a\lambda_3 (C_d \rho A) v \dot{v} = 0 \quad (41)$$

In Equation (41) only \dot{v} can be zero. Therefore, during a potential singular interval the velocity must be a constant. The corresponding input power is obtained using Equation (12),

$$u^* = u_{\dot{v}=0} = mv \left(h(s) + \frac{1}{2m} (C_d \rho A) v^2 \right) \quad (42)$$

which varies with the road grade.

Considering all of the cases discussed above, the optimal power trajectory can only take values from the vector below,

$$u^* = \begin{bmatrix} u_{max} \\ u_{\dot{v}=0} \\ CP \\ 0 \end{bmatrix} \quad (43)$$

Equation (43) provides the *necessary* conditions for optimality of u since it was based on a PMP analysis. It therefore suggests that the global minimizer at each time $u^*(t)$ must be one of these modes. This indicates that the optimal pedaling strategy may include one or more of the four modes of pedaling at maximal power, riding at CP , resting, or riding

at a constant speed. While this insight is useful, it is difficult to analytically determine when the switching between these modes happens. Note that the three state equations along with the three co-state equations form a two point boundary value problem that is generally difficult to solve analytically. The switching dynamics of the problem at hand creates additional challenges. Therefore, next we resort to numerical solution of the optimal control problem via dynamic programming. The above PMP analysis proves valuable in limiting the input space in DP process to only the modes described by Equation (43) which significantly reduces the computational burden of DP.

VII. NUMERICAL SOLUTION OF THE PROBLEM

In our DP implementation, at every step in distance, the state variables are quantized between their minimum and maximum. On the other hand, the control variable u is only quantized at the four power levels in Equation (43) without the loss of optimality, which will significantly reduce the required memory and time of the computing process. First, the state space model in Equation (9) is discretized. Since the final destination is known, we pick distance as the independent variable and discretize it at regular intervals $\Delta s = 10$ m. With a zero-order hold on input in between sampling intervals we obtain the following discretized state-space equations:

$$t_{i+1} = t_i + \frac{\Delta s}{v_i} \quad (44)$$

$$\begin{aligned} v_{i+1} = v_i + \frac{\Delta s}{v_i} \left(\frac{u_i}{m_t v_i} - g(\sin(\theta_i) + \mu \cos(\theta_i)) \right. \\ \left. - \frac{0.5 C_d \rho A}{m_t} v_i^2 \right) \end{aligned} \quad (45)$$

$$\begin{cases} w_{i+1} = w_i - \frac{\Delta s}{v_i} (u_i - CP) & u_i \geq CP \\ w_{i+1} = w_i - \frac{\Delta s}{v_i} (au_i + b - CP) & u_i < CP \end{cases} \quad (46)$$

The cost function in Equation (14) is rewritten with position as the independent variable and discretized as follows¹,

$$J_N = \sum_{i=0}^{i=N} \frac{\Delta s_i}{v_i} \quad (47)$$

According to the Bellman's principle of optimality [82], when a system is on its optimal path from an initial state to a final state, regardless of any past decision or state, it should follow an optimal policy for the remainder of the route. Therefore, in dynamic programming, to find the optimal state trajectory, one can begin from the final state and move backward and calculate the optimal cost-to-go from any state to the final step. Figure 8 demonstrates the backward dynamic

¹When implementing this objective function in DP, we sometimes observed chattering in the power trajectory. This chattering can be the optimal solution or due to the coarse quantization of control input to only four (optimal) modes. To achieve a practical power trajectory for a cyclist, we added a regularization term to the cost that penalizes the change in control input from stage to stage multiplied by a small penalty weight. The weight was carefully tuned to minimize the impact of the regularization term on the value of the objective function.

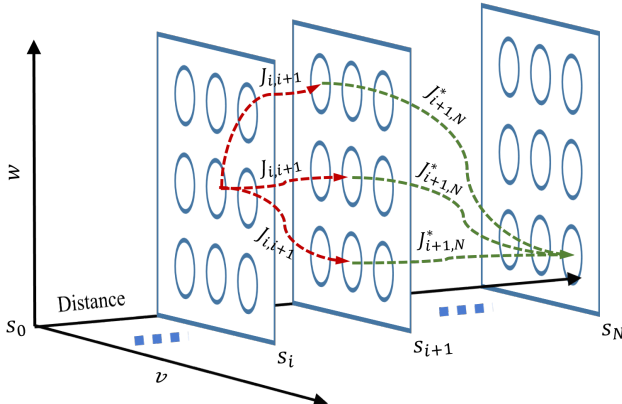


Fig. 8: Demonstration of use of Bellman's principle of optimality in dynamic programming.

programming method based on the Bellman's principle of optimality. The optimal costs from all of the nodes at s_{i+1} to the final state at s_N are stored as $J_{i+1,N}^*$. Then, cost-to-go from every node at s_i to all of the nodes at s_{i+1} is calculated and the optimal value among them is stored at the specified node at s_i . This process is repeated backwards to the beginning of the route. Subsequently, in a forward DP sweep, the optimal action at each discretized state node will be known. Let's denote the optimal cost-to-go from specific velocity and energy states at step s_{i+1} to s_N by $J_{i+1,N}^*$. Then, the optimal trajectory from step s_i to s_N will be,

$$J_{i,N}^* = \min_{u_i} [J_{i,i+1} + J_{i+1,N}^*(x)] \quad (48)$$

where

$$J_{i+1,N}^* = \min_{u_{i+1}, u_{i+2}, \dots, u_{N-1}} [J_{i+1,N}] \quad (49)$$

The DP formulation was then coded in MATLAB. At every step in distance, velocity v is quantized to 300 nodes spaced uniformly in the interval $[1, 20] \text{ m/s}$. The choice of minimum velocity at 1 m/s is because i) speeds closer to zero cause numerical issues as v appears in the denominator in the discretized equations of motion ii) during a time-trial the athlete is unlikely to pedal at lower speeds. Anaerobic energy w is quantized into 600 nodes spread uniformly between 0 and the Sub 14th AWC ($7841J$). As discussed earlier, the input power u is also quantized to 4 nodes the the levels indicated by Equation (43).

When at the distance s_i from the initial position, v_i and w_i states move to v_{i+1} and w_{i+1} by applying an input u_i . The resultant states at step s_{i+1} will not necessarily attain the quantized values of states v and w . Therefore, we implemented a stochastic transition to the neighboring nodes on the $v - w$ plane. In the transition cost is calculated as a weighted summation of the cost at the neighboring nodes, and then stored in the closest node.

Initially, the cyclist starts from the minimum velocity, and his/her remaining energy is initialized at AWC . The DP simulation was ran on a desktop computer with a 3.2GHz Intel core i5 CPU, and 12GB of RAM. The run time for our

longest cycling route (18km) was 53 min and 45 sec. This is thanks to the PMP results that allowed us to significantly reduce the input quantization. Without it the computation time would be several hours.

VIII. RESULTS AND DISCUSSION

A. Simulating Optimal Pacing

To illustrate the nature of optimal solution, we first found the optimal pace over 4 km roads with three basic elevation profiles: a flat road, a road with a 5% grade climb, and a road with two hills. Figure 9 shows the three scenarios and the results based on Sub 14 data. Optimal power u , remaining anaerobic energy w , and velocity v are shown in each case. The figure also shows which one of the four optimal control mode was chosen in the u_{mode} subplot, in which which values of 1, 2, 3, and 4 correspond respectively to the control u equaling, 0, CP , $u_{i=0}$, and u_{max} .

On the flat road, the optimal strategy is to go all-out till all anaerobic reserves are depleted and then continue with critical power. In this case, the maximum power constraint is activated and the power trajectory stays on the constraint. More interestingly, during the ramp course, the optimal pacing strategy benefits from elevation preview. The cyclist burns only 2% of anaerobic energy in the starting line to get to the velocity that can be then maintained by applying CP . The reserved energy comes to use during the ascent over the hill, by the end of which all of the AWC is expended and the cyclist pedals at CP towards the end. During the simulation over a course with two uphill sections, having known about the upcoming downhill, the controller recommends the cyclist to burn most of the anaerobic energy. Then during the downhill, the subject recovers 8% of the AWC to overcome the second hill. In this case, all four modes of optimal power are applied.

B. Baseline Performance Captured by an Experiment

We had the opportunity to simulate the cycling course of the 2019 Duathlon National Championship in Greenville, South Carolina on our CompuTrainer. The elevation profile of this course is presented in Figure 10. We ran this experiment with Sub 14 by requesting the subject to ride with her own strategy as the baseline test². During the test, she was receiving velocity, distance, power, elevation, and heart rate data in real-time via the interface depicted in Figure 4.

The subject managed to finish the course in 34 min 8 sec. However, our DP simulation suggests that if she followed the optimal power provided by the DP, she would have finished the course in 25 min 56 sec. An important observation from this test is that the subject's self strategy lacks consistency in applying power. During the first 5 km of the course in the self-paced scenario, the average power of the cyclists is 230

²One of the shortcomings of utilizing CompuTrainer is that it does not model drag force during a ride. Therefore, the drag term in Equation (45) should be removed. Also, when the subject is riding downhill, the CompuTrainer cannot accelerate the bicycle as would happen on a real road. Therefore, besides removing the negative resistance force due to downhill section of the course, the calibrated resistance force of 15.5 N is added to Equation (45) instead of the drag force. This force is imposed constantly by the CompuTrainer and is set during the calibration process.

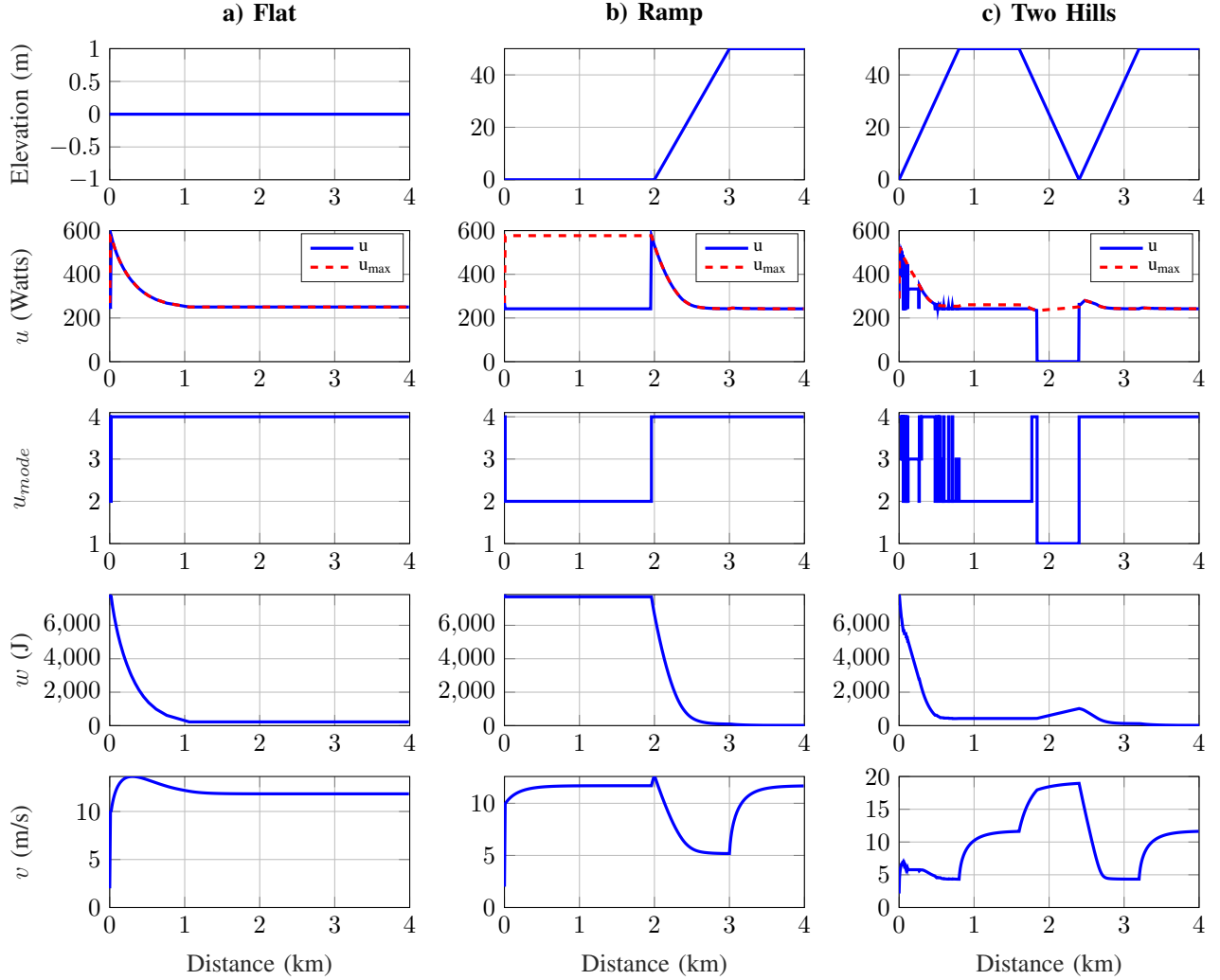


Fig. 9: DP simulation results over three elevation profiles. Sub14 model was used in this set of simulations.

Watts, whereas during the last 5 km it is 190 Watts. Both of these values are below the Subject's critical power (242 Watts). However, the optimal simulation suggests that except for several short periods of maximal effort and recovery, power should remain at CP . While velocity profile in the simulation is always higher than the subject's velocity, both profiles have a similar trend during the course which is dictated by the elevation profile. The difference between the velocity profiles can be explained by the the short frequent maximal efforts that increases the cyclist's velocity. The average power of the optimal strategy is 240 Watts which is only 28 Watts greater than the total average of the self strategy case.

Also, because the cyclist was pedaling below CP for most parts of the course, she recovered almost all of her anaerobic energy at the end which is the against the optimal strategy. Although our subject was familiar with the route and cycles around four times a week, she is not a professional athlete and lacks high level training, which could be one reason for her lack of pace in spending anaerobic energy. Nevertheless, pacing over long hilly courses can be a challenge for professional athletes, and our proposed optimal strategy could be used for coaching or even real-time guidance of

cyclists. The interface depicting in Figure 4 is designed to provide the optimal power in real-time to the cyclist which is the plan of our future work when we can resume testing of human subjects.

IX. CONCLUSIONS & FUTURE WORK

Optimal pacing of a cyclist in a time-trial was formulated as an optimal control problem with an emphasis on the influence of depletion and recovery of anaerobic reserve on performance. In particular each cyclist's maximal power varies with level of fatigue and chosen cadence and plays a critical role in determining the optimal pace in a hilly time-trial. To that end, state-space dynamic models that track depletion and recovery of Anaerobic Work Capacity (AWC) as a function of rider's power above or below their Critical Power (CP) were hypothesized and were validated and calibrated using data from six human subject tests after each spent 14 hours in the lab. In addition, a model was obtained from experimental data relating cyclists' maximal power to their remaining anaerobic capacity and their cadence. With the models in place, we were able to usefully employ Pontryagin's Minimum Principle to determine that over any road profile,

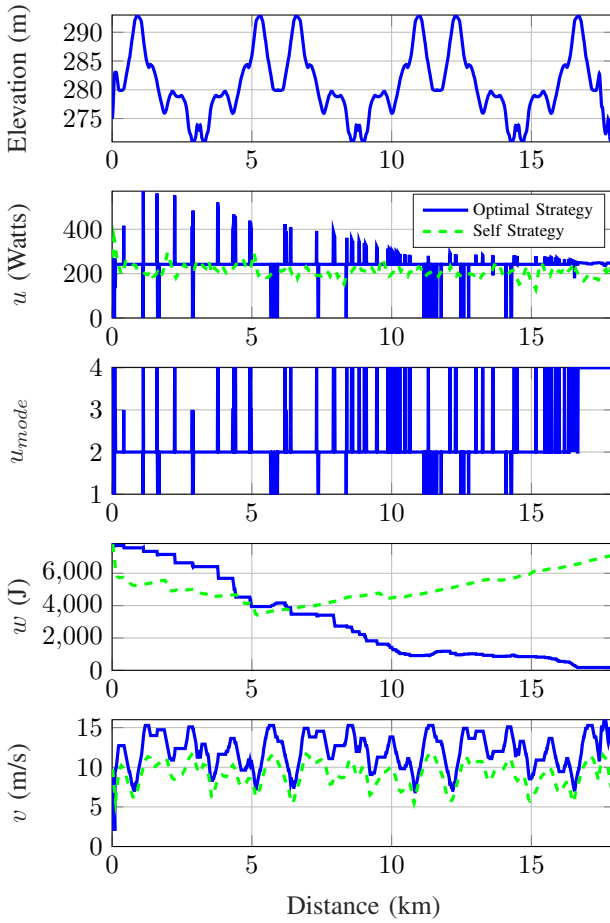


Fig. 10: Power and energy trajectory differences between sub 14's self strategy and the optimal simulation on the Greenville Duathlon course.

the optimal strategy is bang-singular-bang, switching between maximum exertion, no exertion, pedaling at CP , or cruising at constant speeds. Global optimality of these four modes was further verified via the numerical method of Dynamic Programming. Once global optimality was confirmed, limiting the quantization of the cyclist power to only these four optimal modes, substantially reduced the computational load of DP and allowed finer quantization of the states. We demonstrated that the strategy for an 18 km course can be computed in around 2 minutes. Simulations over simple road profiles with one or two steep climbs, showed the efficacy of the optimal strategy in distributing the depletion of AWC along the whole course and appropriately pacing the cyclist in anticipation of climbs. We also simulated human subject 14 over the 2019 Greenville Duathlon course. We had data from subject 14 pedaling the same course on a CompuTrainer with her self-strategy. The simulation suggested that optimal pacing could speed up subject 14 and allow her to finish the course in 76% of her original time (reduction from 2048 seconds to 1556 seconds) with a 28 Watt increase in her average output power which is 11% of her CP . The comparison indicates that consistency in power generation is a key difference between the subject's self and the optimal strategies. While the power should be kept at CP for most of the ride, the cyclist benefits

from frequent short sprints to increase velocity.

We recently completed a pilot test in which subject 14 was instructed to follow a *sub-optimal* strategy displayed to her in real-time and as a result her trial-time improved over self-strategy. We hope to verify that performance can be indeed improved via optimal strategy feedback in repeat experiments once we are able to resume human subject testing in the lab. Other future work include additional 3MT tests at different fatigue and cadence levels to further validate our maximal power surface depicted in Figure 6. A few recent studies [64], [65] suggest that 3MT tests may not provide very accurate estimation of CP and AWC and therefore there is room for additional work on protocols that better estimate these parameters. Our optimal control analysis and strategy do not depend on the value of these parameters and could be exercised with more accurate parameter values.

ACKNOWLEDGMENT

The authors would like to thank Furman University students Frank Lara, Mason Coppi, Nicholas Hayden, Lee Shearer, Brendan Rhim, Alec Whyte, and Jake Ogden for their contribution in data collection from recruited human subjects. Also they would like to thank the fantastic subjects who agreed to do a series of extremely challenging experiments and helped this project progress.

REFERENCES

- [1] F. Ashtiani, V. S. M. Sreedhara, A. Vahidi, R. Hutchison, and G. Mocko, "Experimental modeling of cyclists fatigue and recovery dynamics enabling optimal pacing in a time trial," in *2019 American Control Conference (ACC)*. IEEE, 2019, pp. 5083–5088.
- [2] C. R. Abbiss and P. B. Laursen, "Models to explain fatigue during prolonged endurance cycling," *Sports medicine*, vol. 35, no. 10, pp. 865–898, 2005.
- [3] B. Bigland-Ritchie and J. Woods, "Changes in muscle contractile properties and neural control during human muscular fatigue," *Muscle & nerve*, vol. 7, no. 9, pp. 691–699, 1984.
- [4] R. H. Morton, "The critical power and related whole-body bioenergetic models," *European journal of applied physiology*, vol. 96, no. 4, pp. 339–354, 2006.
- [5] H. C. Bergstrom, T. J. Housh, J. M. Zuniga, D. A. Traylor, R. W. Lewis Jr, C. L. Camic, R. J. Schmidt, and G. O. Johnson, "Differences among estimates of critical power and anaerobic work capacity derived from five mathematical models and the three-minute all-out test," *The Journal of Strength & Conditioning Research*, vol. 28, no. 3, pp. 592–600, 2014.
- [6] G. C. Bogdanis, M. E. Nevill, L. H. Boobis, H. Lakomy, and A. M. Nevill, "Recovery of power output and muscle metabolites following 30 s of maximal sprint cycling in man," *The Journal of physiology*, vol. 482, no. 2, pp. 467–480, 1995.
- [7] S. A. Fayazi, N. Wan, S. Lucich, A. Vahidi, and G. Mocko, "Optimal pacing in a cycling time-trial considering cyclist's fatigue dynamics," in *American Control Conference (ACC), 2013*. IEEE, 2013, pp. 6442–6447.
- [8] N. Wan, S. A. Fayazi, H. Saeidi, and A. Vahidi, "Optimal power management of an electric bicycle based on terrain preview and considering human fatigue dynamics," in *American Control Conference (ACC), 2014*. IEEE, 2014, pp. 3462–3467.
- [9] V. S. M. Sreedhara, F. Ashtiani, G. Mocko, A. Vahidi, and R. Hutchison, "Modeling the recovery of w' in the moderate to heavy exercise intensity domain," *Medicine and Science in Sports and Exercise*, 2020.
- [10] J. De Jong, R. Fokkink, G. J. Olsder, and A. Schwab, "The individual time trial as an optimal control problem," *Proceedings of the Institution of Mechanical Engineers, Part P: Journal of Sports Engineering and Technology*, vol. 231, no. 3, pp. 200–206, 2017.
- [11] N. K. Vollestad, "Measurement of human muscle fatigue," *Journal of Neuroscience Methods*, vol. 74, no. 2, pp. 219–227, 1997.

[12] R. H. Edwards, "Human muscle function and fatigue," *Human muscle fatigue: physiological mechanisms*, pp. 1–18, 1981.

[13] R. M. Enoka and D. G. Stuart, "Neurobiology of muscle fatigue," *Journal of applied physiology*, vol. 72, no. 5, pp. 1631–1648, 1992.

[14] C. S. Fulco, S. F. Lewis, P. N. Frykman, R. Boushel, S. Smith, E. A. Harman, A. Cymerman, and K. B. Pandolf, "Muscle fatigue and exhaustion during dynamic leg exercise in normoxia and hypobaric hypoxia," *Journal of Applied Physiology*, vol. 81, no. 5, pp. 1891–1900, 1996.

[15] D. Kay and F. E. Marino, "Fluid ingestion and exercise hyperthermia: implications for performance, thermoregulation, metabolism and the development of fatigue," *Journal of sports sciences*, vol. 18, no. 2, pp. 71–82, 2000.

[16] D. Kay, F. E. Marino, J. Cannon, A. S. C. Gibson, M. I. Lambert, and T. D. Noakes, "Evidence for neuromuscular fatigue during high-intensity cycling in warm, humid conditions," *European journal of applied physiology*, vol. 84, no. 1-2, pp. 115–121, 2001.

[17] C. Williams and S. Ratel, *Human muscle fatigue*. Routledge, 2009.

[18] J. M. Davis and S. P. Bailey, "Possible mechanisms of central nervous system fatigue during exercise," *Medicine and science in sports and exercise*, vol. 29, no. 1, pp. 45–57, 1997.

[19] J. A. Kent-Braun, "Central and peripheral contributions to muscle fatigue in humans during sustained maximal effort," *European journal of applied physiology and occupational physiology*, vol. 80, no. 1, pp. 57–63, 1999.

[20] R. M. Enoka and J. Duchateau, "Muscle fatigue: what, why and how it influences muscle function," *The Journal of physiology*, vol. 586, no. 1, pp. 11–23, 2008.

[21] J. Liepert, S. Kotterba, M. Tegenthoff, and J.-P. Malin, "Central fatigue assessed by transcranial magnetic stimulation," *Muscle & Nerve: Official Journal of the American Association of Electrodiagnostic Medicine*, vol. 19, no. 11, pp. 1429–1434, 1996.

[22] R. Moussavi, P. Carson, M. Boska, M. Weiner, and R. Miller, "Non-metabolic fatigue in exercising human muscle," *Neurology*, vol. 39, no. 9, pp. 1222–1222, 1989.

[23] B. L. Allman and C. L. Rice, "Neuromuscular fatigue and aging: central and peripheral factors," *Muscle & nerve*, vol. 25, no. 6, pp. 785–796, 2002.

[24] T. Moritani, M. Muro, and A. Nagata, "Intramuscular and surface electromyogram changes during muscle fatigue," *Journal of Applied Physiology*, vol. 60, no. 4, pp. 1179–1185, 1986.

[25] B. Bigland and O. Lippold, "Motor unit activity in the voluntary contraction of human muscle," *The Journal of Physiology*, vol. 125, no. 2, pp. 322–335, 1954.

[26] J. Potvin and L. Bent, "A validation of techniques using surface emg signals from dynamic contractions to quantify muscle fatigue during repetitive tasks," *Journal of Electromyography and Kinesiology*, vol. 7, no. 2, pp. 131–139, 1997.

[27] B. Gerdle, B. Larsson, and S. Karlsson, "Criterion validation of surface emg variables as fatigue indicators using peak torque: a study of repetitive maximum isokinetic knee extensions," *Journal of Electromyography and Kinesiology*, vol. 10, no. 4, pp. 225–232, 2000.

[28] J. E. Hall, *Guyton and Hall textbook of medical physiology e-Book*. Elsevier Health Sciences, 2015.

[29] P. Cerretelli, D. Pendergast, W. Paganelli, and D. Rennie, "Effects of specific muscle training on vo₂ on-response and early blood lactate," *Journal of Applied Physiology*, vol. 47, no. 4, pp. 761–769, 1979.

[30] T. J. Barstow, S. Buchthal, S. Zanconato, and D. Cooper, "Muscle energetics and pulmonary oxygen uptake kinetics during moderate exercise," *Journal of Applied Physiology*, vol. 77, no. 4, pp. 1742–1749, 1994.

[31] B. Saltin and S. Strange, "Maximal oxygen uptake: "old" and "new" arguments for a cardiovascular limitation," *Medicine and science in sports and exercise*, vol. 24, no. 1, pp. 30–37, 1992.

[32] T. J. Barstow, A. M. Jones, P. H. Nguyen, and R. Casaburi, "Influence of muscle fiber type and pedal frequency on oxygen uptake kinetics of heavy exercise," *Journal of Applied Physiology*, vol. 81, no. 4, pp. 1642–1650, 1996.

[33] R. Boushel and C. Piantadosi, "Near-infrared spectroscopy for monitoring muscle oxygenation," *Acta Physiologica Scandinavica*, vol. 168, no. 4, pp. 615–622, 2000.

[34] R. Belardinelli, T. J. Barstow, J. Porszasz, and K. Wasserman, "Changes in skeletal muscle oxygenation during incremental exercise measured with near infrared spectroscopy," *European journal of applied physiology and occupational physiology*, vol. 70, no. 6, pp. 487–492, 1995.

[35] M. C. Van Beekvelt, W. N. Colier, R. A. Wevers, and B. G. Van Engelen, "Performance of near-infrared spectroscopy in measuring local o₂ consumption and blood flow in skeletal muscle," *Journal of Applied Physiology*, vol. 90, no. 2, pp. 511–519, 2001.

[36] Moxy, "Moxy muscle oxygenation monitor," <https://www.moxymonitor.com>.

[37] BSXinsight, "BSXinsight cycling edition," <https://www.bsxinsight.com>.

[38] R. Beneke, "Methodological aspects of maximal lactate steady state—implications for performance testing," *European journal of applied physiology*, vol. 89, no. 1, pp. 95–99, 2003.

[39] V. L. Billat, P. Sirvent, G. Py, J.-P. Koralsztein, and J. Mercier, "The concept of maximal lactate steady state," *Sports medicine*, vol. 33, no. 6, pp. 407–426, 2003.

[40] I. Jacobs, P. Tesch, O. Bar-Or, J. Karlsson, and R. Dotan, "Lactate in human skeletal muscle after 10 and 30 s of supramaximal exercise," *Journal of Applied Physiology*, vol. 55, no. 2, pp. 365–367, 1983.

[41] J. Friel, *The cyclist's training bible*. VeloPress, 2012.

[42] A. V. Hill *et al.*, "Muscular movement in man: The factors governing speed and recovery from fatigue," *Muscular Movement in Man: the Factors governing Speed and Recovery from Fatigue*, 1927.

[43] H. Ishii and Y. Nishida, "Effect of lactate accumulation during exercise-induced muscle fatigue on the sensorimotor cortex," *Journal of physical therapy science*, vol. 25, no. 12, pp. 1637–1642, 2013.

[44] L. Jorfeldt, A. Juhlin-Dannfelt, and J. Karlsson, "Lactate release in relation to tissue lactate in human skeletal muscle during exercise," *Journal of Applied Physiology*, vol. 44, no. 3, pp. 350–352, 1978.

[45] A. Nummela, T. Vuorimaa, and H. Rusko, "Changes in force production, blood lactate and emg activity in the 400-m sprint," *Journal of sports sciences*, vol. 10, no. 3, pp. 217–228, 1992.

[46] M. Aubier, T. Trippenbach, and C. Roussos, "Respiratory muscle fatigue during cardiogenic shock," *Journal of Applied Physiology*, vol. 51, no. 2, pp. 499–508, 1981.

[47] M. Burnley, J. H. Doust, and A. Vanhatalo, "A 3-min all-out test to determine peak oxygen uptake and the maximal steady state," *Medicine & Science in Sports & Exercise*, vol. 38, no. 11, pp. 1995–2003, 2006.

[48] A. Mason, O. Korostynska, J. Louis, L. E. Cordova-Lopez, B. Abdullah, J. Greene, R. Connell, and J. Hopkins, "Noninvasive in-situ measurement of blood lactate using microwave sensors," *IEEE Transactions on Biomedical Engineering*, vol. 65, no. 3, pp. 698–705, 2018.

[49] H. Allen, A. R. Coggan, and S. McGregor, *Training and racing with a power meter*. VeloPress, 2019.

[50] A. S. Welch, A. Hulley, C. Ferguson, and M. R. Beauchamp, "Affective responses of inactive women to a maximal incremental exercise test: A test of the dual-mode model," *Psychology of Sport and Exercise*, vol. 8, no. 4, pp. 401–423, 2007.

[51] D. A. Keir, F. Y. Fontana, T. C. Robertson, J. M. Murias, D. H. Paterson, J. M. Kowalchuk, and S. Pogliaghi, "Exercise intensity thresholds: Identifying the boundaries of sustainable performance," *Medicine and science in sports and exercise*, vol. 47, no. 9, pp. 1932–1940, 2015.

[52] J. S. Pringle and A. M. Jones, "Maximal lactate steady state, critical power and emg during cycling," *European journal of applied physiology*, vol. 88, no. 3, pp. 214–226, 2002.

[53] J. Dekerle, B. Baron, L. Dupont, J. Vanvelcenaher, and P. Pelayo, "Maximal lactate steady state, respiratory compensation threshold and critical power," *European journal of applied physiology*, vol. 89, no. 3-4, pp. 281–288, 2003.

[54] F. Mattioni Maturana, D. A. Keir, K. M. McLay, and J. M. Murias, "Can measures of critical power precisely estimate the maximal metabolic steady-state?" *Applied Physiology, Nutrition, and Metabolism*, vol. 41, no. 11, pp. 1197–1203, 2016.

[55] H. Monod and J. Scherrer, "The work capacity of a synergic muscular group," *Ergonomics*, vol. 8, no. 3, pp. 329–338, 1965.

[56] B. Whipp, D. Huntsman, T. Storer, N. Lamarra, and K. Wasserman, "A constant which determines the duration of tolerance to high-intensity work," in *Federation proceedings*, vol. 41, no. 5. FEDERATION AMER SOC EXP BIOL 9650 ROCKVILLE PIKE, BETHESDA, MD 20814-3998, 1982, pp. 1591–1591.

[57] A. J. Bull, T. J. Housh, G. O. Johnson, and S. R. Perry, "Effect of mathematical modeling on the estimation of critical power," *Medicine & Science in Sports & Exercise*, vol. 32, no. 2, p. 526, 2000.

[58] G. A. Gaesser, T. J. Carnevale, A. Garfinkel, D. O. Walter, and C. J. Womack, "Estimation of critical power with nonlinear and linear models," *Medicine and science in sports and exercise*, vol. 27, no. 10, pp. 1430–1438, 1995.

[59] D. W. Hill, "The critical power concept," *Sports medicine*, vol. 16, no. 4, pp. 237–254, 1993.

[60] D. J. Housh, T. J. Housh, and S. M. Bauge, "A methodological consideration for the determination of critical power and anaerobic work capacity," *Research Quarterly for Exercise and Sport*, vol. 61, no. 4, pp. 406–409, 1990.

[61] A. Vanhatalo, J. H. Doust, and M. Burnley, "Determination of critical power using a 3-min all-out cycling test," *Medicine and science in sports and exercise*, vol. 39, no. 3, pp. 548–555, 2007.

[62] T. M. Johnson, P. J. Sexton, A. M. Placek, S. R. Murray, and R. W. Pettitt, "Reliability analysis of the 3-min all-out exercise test for cycle ergometry," *Medicine and science in sports and exercise*, vol. 43, no. 12, pp. 2375–2380, 2011.

[63] A. Vanhatalo, J. H. Doust, and M. Burnley, "Robustness of a 3 min all-out cycling test to manipulations of power profile and cadence in humans," *Experimental physiology*, vol. 93, no. 3, pp. 383–390, 2008.

[64] J. C. Bartram, D. Thewlis, D. T. Martin, and K. I. Norton, "Predicting critical power in elite cyclists: questioning the validity of the 3-minute all-out test," *International Journal of Sports Physiology and Performance*, vol. 12, no. 6, pp. 783–787, 2017.

[65] J. Wright, S. Bruce-Low, and S. Jobson, "The reliability and validity of the 3-minute all-out cycling critical power test," *International Journal of Sports Medicine*, vol. 38, no. 06, pp. 462–467, 2017.

[66] R. H. Morton and L. V. Billat, "The critical power model for intermittent exercise," *European journal of applied physiology*, vol. 91, no. 2-3, pp. 303–307, 2004.

[67] C. Ferguson, H. B. Rossiter, B. J. Whipp, A. J. Cathcart, S. R. Murgatroyd, and S. A. Ward, "Effect of recovery duration from prior exhaustive exercise on the parameters of the power-duration relationship," *Journal of applied physiology*, vol. 108, no. 4, pp. 866–874, 2010.

[68] P. Bickford, V. S. M. Sreedhara, G. M. Mocko, A. Vahidi, and R. E. Hutchison, "Modeling the expenditure and recovery of anaerobic work capacity in cycling," in *Multidisciplinary Digital Publishing Institute Proceedings*, vol. 2, no. 6, 2018, p. 219.

[69] D. Seck, H. Vandewalle, N. Decrops, and H. Monod, "Maximal power and torque-velocity relationship on a cycle ergometer during the acceleration phase of a single all-out exercise," *European journal of applied physiology and occupational physiology*, vol. 70, no. 2, pp. 161–168, 1995.

[70] A. J. Sargeant, E. Hoinville, and A. Young, "Maximum leg force and power output during short-term dynamic exercise," *Journal of applied physiology*, vol. 51, no. 5, pp. 1175–1182, 1981.

[71] J.-B. Morin and P. Samozino, *Biomechanics of training and testing: innovative concepts and simple field methods*. Springer, 2018.

[72] O. Buttelli, D. Seck, H. Vandewalle, J. Jouanny, and H. Monod, "Effect of fatigue on maximal velocity and maximal torque during short exhausting cycling," *European journal of applied physiology and occupational physiology*, vol. 73, no. 1-2, pp. 175–179, 1996.

[73] B. R. MacIntosh and J. R. Fletcher, "The parabolic power-velocity relationship does apply to fatigued states," *European journal of applied physiology*, vol. 111, no. 2, p. 319, 2011.

[74] R. E. Hutchison, F. Ashtiani, K. S. Edwards, G. A. Klapthor, G. M. Mocko, and A. Vahidi, "Effects of w' depletion on the torque-velocity relationship in cycling," *Medicine and Science in Sports and Exercise*, 2021.

[75] RACERMATE, "Computrainer," <https://www.racermateinc.com/computrainer>.

[76] D. Hartman, "Perfpro studio," <https://perfprostudio.com/>.

[77] R. R. Davison, J. Corbett, and L. Ansley, "Influence of temperature and protocol on the calibration of the computrainer electromagnetically-braked cycling ergometer," *International SportMed Journal*, vol. 10, no. 2, pp. 66–76, 2009.

[78] I. E. Clark, H. E. Gartner, J. L. Williams, and R. W. Pettitt, "Validity of the 3-minute all-out exercise test on the computrainer," *The Journal of Strength & Conditioning Research*, vol. 30, no. 3, pp. 825–829, 2016.

[79] B. Karsten, S. A. Jobson, J. Hopker, L. Stevens, and C. Beedie, "Validity and reliability of critical power field testing," *European journal of applied physiology*, vol. 115, no. 1, pp. 197–204, 2015.

[80] P. F. Skiba, W. Chidnok, A. Vanhatalo, and A. M. Jones, "Modeling the expenditure and reconstitution of work capacity above critical power," *Medicine and science in sports and exercise*, vol. 44, no. 8, p. 1526, 2012.

[81] A. E. Bryson, *Applied optimal control: optimization, estimation and control*. Routledge, 2018.

[82] R. E. Bellman and S. E. Dreyfus, *Applied dynamic programming*. Princeton university press, 2015, vol. 2050.



Faraz Ashtiani is a Ph.D. student of mechanical engineering at Clemson University, SC, USA. He received his B.Sc. in mechanical engineering from University of Tehran, Iran in 2015. His research interests are the applications of optimal control, intelligent transportation systems, and connected and autonomous vehicle technologies.



Vijay Sarthy M Sreedhara Vijay Sarthy M Sreedhara is a Ph.D. candidate of Mechanical Engineering at Clemson University USA. He received his M.Sc. in Mechanical Engineering from Clemson University, USA in 2015 and his B.E. of Engineering degree in Mechanical Engineering from Visvesvaraya Technological University, India in 2009. Prior to graduate school, he has worked as an Engineer at John Deere and Toyota in India. His research interests span the areas of human performance optimization, engineering of sport, and product design

and development.



Ardalan Vahidi is a Professor of Mechanical Engineering at Clemson University, South Carolina. He received his Ph.D. in mechanical engineering from the University of Michigan, Ann Arbor, in 2005, M.Sc. in transportation safety from George Washington University, Washington DC, in 2002, and B.S. and M.Sc. in civil engineering from Sharif University, Tehran in 1996 and 1998, respectively. In 2012–2013 he was a Visiting Scholar at the University of California, Berkeley. He has also held scientific visiting positions at BMW Technology Office in California, and at IFP Energies Nouvelles, in France. His research is at the intersection of energy, vehicular systems, and automatic control. His recent publications span topics in alternative vehicle powertrains, intelligent transportation systems, and connected and autonomous vehicle technologies.



Randolph Hutchison received the B.S. degree in aerospace engineering from Virginia Tech University, Blacksburg, VA, USA, in 1999, and both the M.S. and Ph.D. degrees in bioengineering from Clemson University, Clemson, SC, USA, in 2011. He has held positions at Pratt & Whitney Aircraft Engines as a turbine designer in structural vibrations and aerodynamics in West Palm Beach, FL, and North Haven, CT, USA. He is currently an Associate Professor at Furman University in the Department of Health Sciences, Greenville, SC, USA. His research interests include biomechanical and physiological modeling to optimize human locomotion with the use of wearable sensors. His recent publications span topics in validation of sensors for the measurement of human motion, biomechanics-based orthopaedic rehabilitation, and evaluation of novel power-based training programs.



Gregory Mocko is currently an Associated Professor in mechanical engineering at Clemson University Clemson SC USA. He received the B.Sc. degree in mechanical engineering and material Science from University of Connecticut, Storrs, CT USA in 1999, M.Sc. degree in mechanical engineering from Oregon State University, Corvallis, OR USA in 2001 and Ph.D. in mechanical engineering from the Georgia Institute of Technology, Atlanta GA USA in 2006. His research interests are broad including human performance, teaming and communication within complex design, and knowledge-based manufacturing. His recent publications include energy expenditure during physical activities, simulation of manufacturing processes, and retrieval of knowledge to support design and manufacturing.